Decentralised Navigation and Collision Avoidance for Aircraft in 3D Space

Giannis Roussos and Kostas J. Kyriakopoulos

Abstract— We present an algorithm for the distributed navigation of nonholonomic aircraft-like agents in 3D space. The proposed control scheme offers improved applicability for aircraft navigation and compatibility with ATC practice wrt previous work. The algorithm maintains a desired horizontal velocity, while limiting the climb or descent angle within predefined bounds. Moreover, it is designed to favor straight and level flight, yielding more sensible manoeuvres that require reduced steering effort. Simulation results demonstrate the performance of the approach.

I. INTRODUCTION

Automation in Air Traffic Control (ATC) is drawing increasing attention during the last years. Growing air traffic levels call for a new way to handle tasks in ATC, as the current airspace structure and the centralised ATM model currently used will not be able to cope with future air traffic. Moreover, as Unmanned Aerial Vehicles (UAVs) are becoming increasingly popular, some form of automation is required to allow their safe integration in air traffic.

Conflict Detection and Resolution (CD&R) is a critical function within ATC, and is divided into three levels [1]:

- Long-term, i.e. flow management in a horizon of hours.
- Mid-term, where collision-free trajectories are derived for a horizon of tenths of minutes.
- Short-term, handling collisions 5 to 10 minutes away.

Optimisation wrt area congestion, fuel efficiency, arrival time, passenger comfort, etc., is usually employed in Long and Mid-term CD&R. Such approaches can yield very good results, but often require considerable time, while performance is not always verified. Short-term CD&R on the other hand, requires guaranteed performance to handle flight safety, and fast response, to allow real time application.

Decentralisation is a key aspect in future air traffic systems, investigated in project iFLY [1]. A centralised system is usually able to offer globally optimal solutions, but requires many computational resources and communication. Decentralised methods are more efficient and tolerant with respect to localised faults. Because of the safety critical role of Short-term CD&R and the limited resources of aircraft, decentralised methods are preferred in this level of CD&R.

This paper considers the control of multiple autonomous fixed-wing aircraft flying in 3D space, while avoiding collisions. The Navigation Functions (NFs) [2] framework is employed in an algorithm that is applicable in ATC. We

Giannis Roussos and Kostas J. Kyriakopoulos are with the Control Systems Lab, Department of Mechanical Engineering, National Technical University of Athens, 9 Heroon Polytechniou Street, Zografou 15780, Greece. email: {jrous, kkyria}@mail.ntua.gr

exploit previous results [3] to build a control scheme that respects the aircraft's capabilities and complies with current ATC practice. Our aim is to avoid complex and erratic maneuvers, as they increase the pilots' workload, prevent human Air Traffic Controllers from maintaining good situation awareness and reduce fuel efficiency and passenger comfort.

In our previous work [3] an augmented 3D unicycle model with the linear velocity and three rotation rates as control inputs was used. In this work we use the horizontal speed, the heading rotation rate and the vertical speed (rate of climb or descent in ATC terms) as control inputs. Essentially, this corresponds to a planar unicycle with the addition of the vertical speed. Such a kinematic model is not limited to aircraft, but can also apply to certain underwater vehicles [4]. Its use here allows three major improvements wrt [3]:

- The set of controls is native to ATC applications, where vertical maneuvering is described by the vertical velocity rather than the elevation angle.
- Vertical and horizontal maneuvering are decoupled, allowing level flight when vertical speed is not needed. This yields simpler, more predictable manoeuvres.
- With the proposed control law, the maximum climb and descent slope can be independently bounded.

Other work on constant velocity collision avoidance includes optimisation solutions, using non-cooperative (worst case) schemes [5], or decentralized, cooperative approaches [6], [7], as well as geometric algorithms [8]. Although the formulation of the collision avoidance problem as an optimisation problem can yield efficient solutions, large computational resources are usually required, making optimisation more relevant to centralised implementations and higher CD&R levels (Long- and Mid-term). [8] uses the intuitive collision cone concept, but requires conflict-free initial conditions to guarantee collision avoidance.

The rest of the paper is organised as follows: section II formulates the problem we treat, followed by a brief introduction to Dipolar Navigation Functions in section III. The proposed control scheme is presented in section IV, while section VI provides simulation results for our algorithm. Section VII summarizes our conclusions.

II. SYSTEM AND PROBLEM DEFINITION

We use the following kinematic model for each agent i:

$$\dot{\boldsymbol{n}}_i = \left[\begin{array}{c} \dot{x}_i \\ \dot{y}_i \end{array} \right] = \mathbf{J}_i \cdot u_i,$$
$$\dot{z}_i = w_i, \qquad (1)$$
$$\dot{\phi}_i = \omega_i,$$
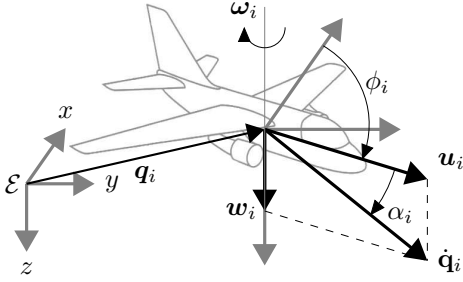
Fig. 1. Model Coordinates $\mathbf{q_i} = [x_i \; y_i \; z_i]^\top$, ϕ_i and controls u_i, w_i, ω_i. Descent angle α_i and vertical velocity w_i shown negative during descent.

where $\boldsymbol{q}_i = \begin{bmatrix} x_i & y_i & z_i \end{bmatrix}^\top$ is the position vector wrt an earth-fixed frame $\mathcal{E}$ (Figure 1), $\boldsymbol{J}_i = \begin{bmatrix} \cos(\phi_i) & \sin(\phi_i) \end{bmatrix}^\top$, $\boldsymbol{n}_i = \begin{bmatrix} x_i & y_i \end{bmatrix}^\top$ is the projection of the agent's position on the horizontal $x - y$ plane, z_i its altitude and ϕ_i the heading angle, i.e. the angle between the agent's longitudinal axis and x axis. The control vector comprises the horizontal velocity u_i, vertical velocity w_i and the angular heading velocity ω_i. This model is a unicycle on the $x - y$ plane, augmented with the vertical velocity w_i adjusting the altitude z_i. We define the climb or descent angle α_i, between the resultant velocity vector $\dot{\boldsymbol{q}}_i = \begin{bmatrix} \dot{x}_i & \dot{y}_i & \dot{z}_i \end{bmatrix}^\top$ and the horizontal $x - y$ plane, $\alpha_i = \tan^{-1}\left(\frac{w_i}{|u_i|}\right)$. Positive α_i represents climbing.

Compared to the model used in [3], (1) decouples horizontal and vertical maneuvering, allowing independent regulation of the vertical velocity. We do not consider the pitch and roll angles or the aircraft dynamics here. We assume that the low level control systems, i.e. avionics onboard the aircraft, will control the pitch and roll angles to achieve the desired linear and angular velocities (u_i, w_i and ω_i respectively).

A. Problem Statement

We address the decentralised navigation of a group of agents described by (1), to their destinations $\boldsymbol{n}_{id} = \begin{bmatrix} x_{id} & y_{id} \end{bmatrix}^\top$ and altitude z_{id}, with heading angle ϕ_{id}. Each agent has a desired absolute horizontal speed $u_{d_i} > 0$, that can be constant, or regulated independently of our algorithm (e.g. u_{d_i} can be the optimal cruising speed for the current altitude), and maximum climb and descent angles $\alpha_{iC} > 0$, $\alpha_{iD} < 0$, respectively. Our aim is to use the desired speed u_{id} for as long as possible, and ensure that all agents respect the above climb and descent angle bounds, i.e. $\alpha_{iD} \leq \alpha_i \leq \alpha_{iC}$.

III. DIPOLAR NAVIGATION FUNCTIONS

Navigation Functions are artificial potential fields, introduced by Rimon and Koditschek [2] for robot navigation. *Dipolar Navigation Functions* [9] employ an additional artificial obstacle H_{nh_i} to better handle non-holonomic agents, yielding trajectories tangent to the target orientation at the destination and avoiding in-place rotation. Thus, each agent is driven to its target with the desired orientation.

Such a Dipolar Navigation Function is of the form:

$$\Phi_i = \frac{\gamma_{di} + f_i}{\left((\gamma_{di} + f_i)^k + H_{nh_i} \cdot G_i \cdot \beta_{0_i}\right)^{1/k}}, \qquad (2)$$

G_i captures all possible collisions involving agent i: G_i is zero when the ith agent participates in a conflict, and positive otherwise. γ_{di} is the goal function, fading at the destination q_{id}. Function $f_i = f_i(G_i)$ enables cooperation between neighboring agents, while β_{0i} bounds agents in the spherical workspace. The artificial obstacle H_{nhi} renders the potential field dipolar. Finally, k is a positive tuning parameter. More details on the construction of Φ_i can be found in [10].

Navigation Function (2) provides almost global convergence to the agents' destinations, along with guaranteed collision avoidance [11]. The potential of such a Navigation Function in a 2D workspace with two obstacles O_1, O_2 is shown in Figure 2. The target is $\begin{bmatrix} x_d & y_d \end{bmatrix} = \begin{bmatrix} 7 & 0 \end{bmatrix}$, with orientation $\phi_d = 0$ and the corresponding nonholonomic obstacle H is the line $x = 7$.
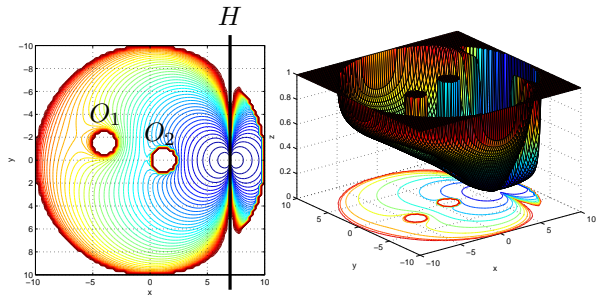

Fig. 2. 2D Dipolar Navigation Function

IV. 3D AIRCRAFT NAVIGATION

A. Preliminaries

The motivation for the proposed control scheme is to produce trajectories that are compatible with the aircraft characteristics and constraints, as well as with current ATM practice. Thus, we develop a control logic that yields more sensible maneuvres than [12], while still maintaining the formal guarantees for collision avoidance and stabilization. The control scheme we suggest relies on a dipolar NF, Φ_i (2) to ensure safety and convergence. We employ the gradient $\nabla_i \Phi_i = \frac{\partial \Phi_i}{\partial \boldsymbol{q}_i} = \begin{bmatrix} \Phi_{ix} & \Phi_{iy} & \Phi_{iz} \end{bmatrix}^\top$ of Φ_j wrt agent's i position $\boldsymbol{q}_i$, where $\Phi_{ix} = \frac{\partial \Phi_i}{\partial x_i}$, etc. As $\nabla_i \Phi_i$ is expressed in earth-fixed coordinates, we use its projection on the agent's i longitudinal (heading) direction: $P_i = \boldsymbol{J}_i^\top \cdot \begin{bmatrix} \Phi_{ix} & \Phi_{iy} \end{bmatrix}^\top$. The sign of P_i, $s_i = \text{sgn}(P_i)$, determines the direction of motion on the horizontal plane, where:

$$\text{sgn}(x) \triangleq \begin{cases} 1, & \text{if } x \geq 0 \\ -1, & \text{if } x < 0. \end{cases}$$

The control law for the vertical velocity w_i depends on the elevation angle of the negated gradient, i.e. the angle between $-\nabla_i \Phi_i$ and the horizontal plane: $\alpha_{\mathbf{nh}i} = -\tan^{-1}\left(\frac{\Phi_{iz}}{\sqrt{\Phi_{ix}^2 + \Phi_{iy}^2}}\right)$. Since $\alpha_{\mathbf{nh}i}$ can take any value in $\left(-\frac{\pi}{2}, \frac{\pi}{2}\right)$, we bound the reference elevation angle $\tilde{\alpha}_i$, within

the agent's feasible climb and descent angles:

$$\tilde{\alpha}_i = \begin{cases} \alpha_{iD}, & \alpha_{\mathbf{nh}i} < \alpha_{iD} \\ \alpha_{\mathbf{nh}i}, & \alpha_{iD} \le \alpha_{\mathbf{nh}i} \le \alpha_{iC} \\ \alpha_{iC}, & \alpha_{\mathbf{nh}i} > \alpha_{iC}. \end{cases}$$

The corresponding reference slope $\tilde{t}_i$ is $\tilde{t}_i = \tan \tilde{\alpha}_i$.
For the design of the control scheme we use three criteria:

1) Safety and Stability: Ensuring a decreasing rate for potential Φ_i is crucial to guarantee convergence and collision avoidance. The time derivative of Φ_i can be written

$$\dot{\Phi}_i = \sum_{j=1}^{N} \nabla_j \Phi_i^{\top} \dot{\boldsymbol{q}}_j = P_i u_i + \Phi_{iz} w_i + \frac{\partial \Phi_i}{\partial t},$$

where the partial derivative $\frac{\partial \Phi_i}{\partial t}$ sums the effect of all but the ith agents' motion on Φ_i: $\frac{\partial \Phi_i}{\partial t} = \sum_{j \ne i} \nabla_j \Phi_i^{\top} \cdot \begin{bmatrix} u_j \boldsymbol{J}_j \\ w_j \end{bmatrix}$.
This criterion is encoded into the continuous switch

$$\sigma_{\Phi i} = \text{sat}\left(\frac{|u_i| \left(\tilde{t}_i \Phi_{iz} - |P_i| + \varepsilon \right) + \frac{\partial \Phi_i}{\partial t}}{|u_i| \tilde{t}_i \Phi_{iz}} \right) \quad (3)$$

where $\text{sat}(x) = \begin{cases} 0, & x < 0 \\ x, & 0 \le x \le 1 \\ 1, & x > 1 \end{cases}$,

and ε is a small positive constant. Thus, $\sigma_{\Phi i}$ is:

- 1 when horizontal velocity u_i ensures that $\dot{\Phi} < -|u_i|\varepsilon$,
- 0 when u_i and $w_i = \tilde{t}_i u_i$ can maintain $\dot{\Phi}_i > -|u_i|\varepsilon$,
- $0 < \sigma_{\Phi i} < 1$ when u_i together with a nonzero vertical velocity w_i, where $|w_i| < |\tilde{t}| u_i$, yields $\dot{\Phi}_i \le -|u_i|\varepsilon$.

2) Horizontal distance from target: For each agent i we define the vertical Target Cylinder (TC) around its destination $\boldsymbol{n}_{id}$, as shown in Figure 3: $\mathcal{C}_i = \{ \boldsymbol{n}_i \mid \|\boldsymbol{n}_i - \boldsymbol{n}_{id}\| \le c_i \}$. $\mathcal{C}_i$ is surrounded by a belt zone $\mathcal{B}_i$ of thickness b_i, $\mathcal{B}_i = \{ \boldsymbol{n}_i \mid c_i < \|\boldsymbol{n}_i - \boldsymbol{n}_{id}\| \le c_i + b_i \}$, while the space outside $\mathcal{C}_i$ and $\mathcal{B}_i$ is the Maneuvering Space $\mathcal{R}_i$: $\mathcal{R}_i = \{ \boldsymbol{n}_i \mid \|\boldsymbol{n}_i - \boldsymbol{n}_{id}\| > c_i + t_i \}$. Finally, let us define the Target Sphere $\mathcal{S}_i$, completely contained in $\mathcal{C}_i$: $\mathcal{S}_i = \{ \boldsymbol{q}_i \mid \|\boldsymbol{q}_i - \boldsymbol{q}_{id}\| \le c_i \}$. The proposed control strategy uses different control schemes in $\mathcal{C}_i$, $\mathcal{B}_i$ and $\mathcal{R}_i$. Inside $\mathcal{R}_i$, the main objective of each agent i is to maneuvre away from collisions and towards the direction of the negated gradient $-\nabla_i \Phi_i$, while maintaining horizontal speed u_{id} and horizontal flight ($w_i = 0$) for as long as possible (i.e. when safety and stability are ensured). Following exactly the slope of $-\nabla_i \Phi_i$ is not required in $\mathcal{R}_i$. Inside $\mathcal{C}_i$ the horizontal speed u_i is gradually reduced, while the vertical velocity w_i follows the gradient's slope, so that each agent converges to its target $\boldsymbol{q}_{id}$. The belt zone $\mathcal{B}_i$ ensures continuous control inputs on the transition between $\mathcal{C}_i$ and $\mathcal{R}_i$. The complete notion is captured by the switch σ_{ni}, plotted in Figure 3:

$$\sigma_{ni} = \text{sat}\left(\frac{\|\boldsymbol{n}_i - \boldsymbol{n}_{id}\| - c_i}{b_i} \right), \quad (4)$$

so that $\sigma_{ni} = \begin{cases} 0, & \boldsymbol{n}_i \in \mathcal{C}_i \\ 1, & \boldsymbol{n}_i \in \mathcal{R}_i \\ a \in (0, 1], & \boldsymbol{n}_i \in \mathcal{B}_i. \end{cases}$
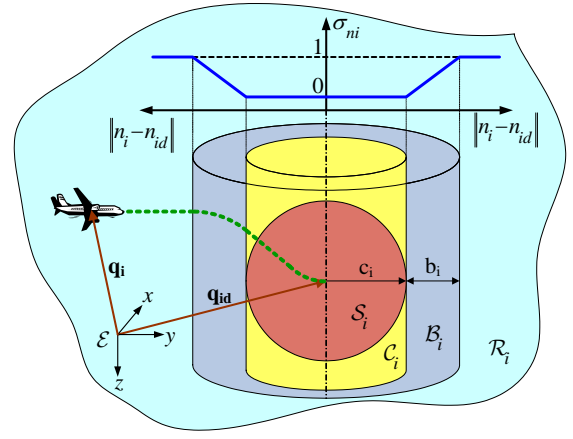

Fig. 3. Target Cylinder $\mathcal{C}_i$, Target Sphere $\mathcal{S}_i$, Belt Zone $\mathcal{B}_i$ and Maneuvering Space $\mathcal{R}_i$ around the target $\boldsymbol{q}_{id}$. σ_{ni} varies linearly in $\mathcal{B}_i$.
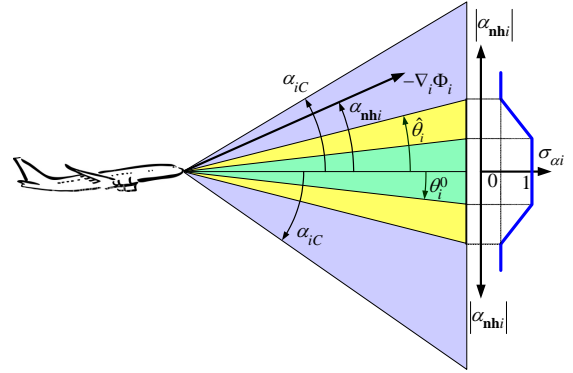
Fig. 4. Angle parameters $\hat{\theta}$, θ_i^0, aircraft limits α_{iC}, α_{iD} and switch $\sigma_{\alpha i}$ with respect to the gradient elevation angle $\alpha_{\mathbf{nh}i}$.

An agent may be driven by the potential's gradient to enter its TC and exit afterwards. As it is shown in the stability analysis though, this does not affect the performance of the algorithm, since all agents eventually stay in their TCs.

3) Elevation angle of the negated gradient: the agents are allowed to fly horizontally only when the absolute elevation angle of $-\nabla_i \Phi_i$, $|\alpha_{\mathbf{nh}i}|$ is lower than a high bound θ_i^0. When $|\alpha_{\mathbf{nh}i}| > \theta_i^0$, vertical maneuvering via w_i is gradually activated, until $|\alpha_{\mathbf{nh}i}| = \hat{\theta}_i > \theta_i^0$, where w_i is used to yield a resultant velocity $\dot{\boldsymbol{q}}_i$ matching exactly the reference elevation angle $\tilde{\alpha}_i$. This is realised via the switch $\sigma_{\alpha i}$ (Fig 4):

$$\sigma_{\alpha i} = \text{sat}\left(\frac{\hat{\theta}_i - |\alpha_{\mathbf{nh}i}|}{\hat{\theta}_i - \theta_i^0} \right).$$

where $\min(\alpha_{iC}, |\alpha_{iD}|) \ge \hat{\theta}_i > \theta_i^0 > 0$. Thus, $\sigma_{\alpha i}$ is:

- 0 when $|\alpha_{\mathbf{nh}i}| \ge \hat{\theta}_i$,
- 1 when $|\alpha_{\mathbf{nh}i}| \le \theta_i^0$, and
- $0 < \sigma_{\alpha i} < 1$ when $\theta_i^0 < |\alpha_{\mathbf{nh}i}| < \hat{\theta}_i$.

B. Control Scheme

The control logic is built around the following principles:

- A nominal absolute speed U_i is used for u_i regulation. U_i is equal to the desired absolute horizontal speed u_{id}

when $q_i \notin \mathcal{S}_i$, i.e. when agent i is more than c_i away from its target, while it is continuously reduced to 0, as the agent approaches its target inside $\mathcal{S}_i$.

- The absolute horizontal velocity $|u_i|$ is kept equal to the nominal signal U_i when $\frac{\partial \Phi_i}{\partial t} \leq U_i \left(|P_i| - \tilde{t}_i \Phi_{iz} - \varepsilon\right)$, i.e. the combination of horizontal and vertical velocities $s_i U_i$ and $U_i \tilde{t}_i$, respectively, can maintain $\dot{\Phi}_i \leq U_i \varepsilon$.

- Vertical velocity w_i is kept zero when all three of the criteria described above are met, i.e.:
  1) Agent i is in its maneuvering zone, $\boldsymbol{n}_i \in \mathcal{R}_i$.
  2) Horizontal speed u_i yields $\dot{\Phi} = P_i u_i + \frac{\partial \Phi_i}{\partial t} \leq -U_i \varepsilon$.
  3) The gradient's absolute elevation angle is at most θ_i^0, $|\alpha_{\mathbf{nh}i}| \leq \theta_i^0$.

  Thus, $w_i = 0$ only when $\sigma_{ni} = \sigma_{\Phi i} = \sigma_{\alpha i} = 1$.

- When safety and stability are at risk, vertical maneuvering via w_i is used up to an elevation slope $\tilde{t}_i$, by setting $w_i = \tilde{t}_i u_i$. If this alone is not enough to achieve $\dot{\Phi}_i \leq U_i \varepsilon$, the magnitudes of both linear velocities are increased in a continuous way to achieve $\dot{\Phi}_i = |u_i| \varepsilon$.

- Agent's i slope is made equal to $\tilde{t}_i$ when any of $\sigma_{\Phi i}$, σ_{ni}, $\sigma_{\alpha i}$ become zero, i.e. any of the following hold:
  1) Agent i is in its TC, $\boldsymbol{n}_i \in \mathcal{C}_i$.
  2) The combination of horizontal speed U_i and vertical speed $\tilde{t}_i U_i$ does not satisfy $\dot{\Phi}_i \leq -U_i \varepsilon$, i.e. $U_i P_i + U_i \tilde{t}_i \Phi_{iz} + \frac{\partial \Phi_i}{\partial t} \geq -U_i \varepsilon$.
  3) The gradient's absolute elevation angle is at least $\hat{\theta}_i$, $|\alpha_{\mathbf{nh}i}| \geq \hat{\theta}_i$.

- Heading angular velocity ω_i uses the control scheme presented in [3] to steer each agent towards the heading angle of $\text{sgn}(P_i)\nabla_i \Phi_i$ and keep control effort low.

Based on these principles, we propose the following control scheme for the linear velocities u_i and w_i of each agent i:

$$u_i = \begin{cases} -s_i U_i, & \frac{\partial \Phi_i}{\partial t} \leq U_i \left(|P_i| - \tilde{t}_i \Phi_{iz} - \varepsilon\right) \\ -s_i \frac{U_i \varepsilon + \frac{\partial \Phi_i}{\partial t}}{|P_i| - \tilde{t}_i \Phi_{iz}}, & \frac{\partial \Phi_i}{\partial t} > U_i \left(|P_i| - \tilde{t}_i \Phi_{iz} - \varepsilon\right) \end{cases} \quad (5a)$$

$$w_i = \left(1 - \min\left(\sigma_{\Phi i}, \sigma_{ni}, \sigma_{\alpha i}\right)\right) \tilde{t}_i |u_i|. \quad (5b)$$

The magnitude $|u_i|$ increases in the second case of (5a), while the transition is continuous by construction:
$\frac{\partial \Phi_i}{\partial t} > U_i \left(|P_i| - \tilde{t}_i \Phi_{iz} - \varepsilon\right) \Rightarrow \frac{U_i \varepsilon + \frac{\partial \Phi_i}{\partial t}}{|P_i| - \tilde{t}_i \Phi_{iz}} > U_i$.
The nominal absolute horizontal velocity U_i is

$$U_i = \begin{cases} u_{id}, & \boldsymbol{n}_i \notin \mathcal{C}_i \\ \frac{\|\boldsymbol{q}_i - \boldsymbol{n}_{id}\|}{c_i} \cdot u_{id}, & \boldsymbol{n}_i \in \mathcal{C}_i. \end{cases} \quad (6)$$

The angular velocity ω_i is given by:

$$\omega_i = \begin{cases} 0, & M_i \geq \varepsilon_\phi \\ \Omega_i \cdot \left(1 - \frac{M_i}{\varepsilon_\phi}\right), & 0 < M_i < \varepsilon_\phi \\ \Omega_i, & M_i \leq 0, \end{cases} \quad (7)$$

where $M_i \triangleq \dot{\phi}_{\boldsymbol{nh}i} (\phi_i - \phi_{\boldsymbol{nh}i})$ and $\Omega_i \triangleq -k_\phi (\phi_i - \phi_{\boldsymbol{nh}i}) + \dot{\phi}_{\boldsymbol{nh}i}$. The *nonholonomic* heading angle $\phi_{\mathbf{nh}i}$ represents the heading of $\text{sgn}(p_i)\nabla_i \Phi_i$:

$$\phi_{\mathbf{nh}i} \triangleq atan2\left(\text{sgn}(p_i)\Phi_{iy}, \text{sgn}(p_i)\Phi_{ix}\right), \quad (8)$$

where $atan2(y, x) \triangleq \arg(x, y)$, $(x, y) \in \mathbb{C}$ and $p_i = \mathbf{J}_{id}^\top \cdot (\boldsymbol{n}_{i1} - \boldsymbol{n}_{i1d})$ is the position vector wrt the destination, projected on the longitudinal axis of the desired orientation. Finally, ε_ϕ is a small positive constant and k_ϕ a positive gain.

To ensure the continuity of $\phi_{\mathbf{nh}i}$ on the destination, where $\nabla_i \Phi_i = 0$, we use the following approximation scheme [13]:

$$\hat{\phi}_{\mathbf{nh}i} \triangleq \begin{cases} \phi_{\mathbf{nh}i}, & \rho_i > \epsilon \\ \frac{\phi_{\mathbf{nh}i}\left(-2\rho_i^3 + 3\epsilon\rho_i^2\right) + \phi_{id}\left(-2(\epsilon-\rho_i)^3 + 3\epsilon(\epsilon-\rho_i)^2\right)}{\epsilon^3}, & \rho_i \leq \epsilon \end{cases}$$

where $\rho_i = \sqrt{\Phi_{ix}^2 + \Phi_{iy}^2}$ and ϵ a small positive constant. Thus, $\hat{\phi}_{\mathbf{nh}i}$ is continuous when $\rho_i = 0$, where $\boldsymbol{q}_i = \boldsymbol{q}_{id}$:
$$\hat{\phi}_{\mathbf{nh}i}(\boldsymbol{q}_{id}) = \lim_{\boldsymbol{q}_i \to \boldsymbol{q}_{id}} \hat{\phi}_{\mathbf{nh}i} = \lim_{\rho_i \to 0} \hat{\phi}_{\mathbf{nh}i} = \hat{\phi}_{\mathbf{nh}i}\Big|_{\rho_i=0} = \phi_{id}$$

V. SAFETY AND STABILITY ANALYSIS

Theorem 1: A team of agents described by (1) under the control law (5) remains always *safe*, i.e. no collisions occur.

Proof: Since agents are considered spherical, collisions can only by translation. Thus, to ensure collision avoidance, it suffices to show that each agent i uses its linear velocities u_i, w_i to stay away from its neighbors. By construction, a Navigation Function is uniformly maximum on the boundary of other agents and its negated gradient points away from them. By the definition of $\alpha_{\mathbf{nh}i}$, $\tilde{\alpha}_i$ and $\tilde{t}_i$, one can verify that $\tilde{t}_i \Phi_{iz} \leq 0$. From the control law (5a), we derive that $P_i u_i \leq -P_i s_i U_i = -|P_i| U_i \leq 0$. Additionally, (5b) yields $\Phi_{iz} w_i = \tilde{t}_i \Phi_{iz} \left(1 - \min\left(\sigma_{\Phi i}, \sigma_{ni}, \sigma_{\alpha i}\right)\right) |u_i| \leq 0$. Consequently, we deduce: $\nabla_i \Phi_i^\top \cdot \dot{\boldsymbol{q}}_i = P_i u_i + \Phi_{iz} w_i \leq 0$. Consider a group of agents, initially far apart from each other so that $\Phi_i|_{t=0} < 1 \quad \forall i$. As Φ_i is continuous and differentiable in space, a collision would imply that at least one colliding agent i moved towards the direction of $\nabla_i \Phi_i$, causing Φ_i to attain its maximum value of 1. This cannot hold, as $\nabla_i \Phi_i^\top \cdot \dot{\boldsymbol{q}}_i \leq 0$, therefore no collisions can occur under control law (5). ∎

Theorem 2: Each agent i described by (1) under the control laws (5), (7) is asymptotically stabilised to its target $\boldsymbol{q}_{id}$ with the desired heading angle ϕ_{id}.

Proof: We employ the candidate Lyapunov function:

$$V = \sum_{i=1}^N V_i, \quad V_i = \Phi_i + \frac{1}{2}\left(\phi_i - \phi_{\mathbf{nh}i}\right)^2. \quad (9)$$

We consider the complete multiagent system $\dot{\mathbf{x}} = f(\mathbf{x})$:
$\mathbf{x} = \left[\boldsymbol{q}_1^\top \dots \boldsymbol{q}_N^\top \ \phi_1 \dots \phi_N \ \phi_{\mathbf{nh}1} \dots \phi_{\mathbf{nh}N}\right]^\top$,
$f(\mathbf{x}) = \left[u_1 \cdot \mathbf{J}_1^\top \ w_1 \dots u_N \cdot \mathbf{J}_N^\top \ w_N \ \omega_1 \dots \omega_N \ \dot{\phi}_{\mathbf{nh}1} \dots \dot{\phi}_{\mathbf{nh}N}\right]^\top$
In order to use the chain rule in [14], we use the Filippov set [15] $K[f(\mathbf{x})]$ and the generalised derivative [16] of $V(\mathbf{x})$:

$$K[f] = \begin{bmatrix} K[u_1]\mathbf{J}_1 \\ K[w_1] \\ \vdots \\ K[u_N]\mathbf{J}_N \\ K[w_N] \\ \omega_1 \\ \vdots \\ \omega_N \\ \dot{\phi}_{\mathbf{nh}1} \\ \vdots \\ \dot{\phi}_{\mathbf{nh}N} \end{bmatrix} \quad \partial V = \begin{bmatrix} \sum_i \nabla_1 \Phi_i \\ \vdots \\ \sum_i \nabla_N \Phi_i \\ (\phi_1 - \phi_{\mathbf{nh}1}) \\ \vdots \\ (\phi_N - \phi_{\mathbf{nh}N}) \\ -(\phi_1 - \phi_{\mathbf{nh}1}) \\ \vdots \\ -(\phi_N - \phi_{\mathbf{nh}N}) \end{bmatrix}.$$

Thus, we calculate the generalised time derivative of $V(\mathbf{x})$:

$$\dot{\tilde{V}} = \bigcap_{\xi \in \partial V} \xi^\top K[f] =$$

$$= \sum_i^N \sum_j^N K[u_i] \nabla_i \Phi_j^\top \begin{bmatrix} \boldsymbol{J}_i \\ 0 \end{bmatrix} + \sum_i^N \sum_j^N K[w_i] \frac{\partial \Phi_j}{\partial z_i} +$$

$$+ \sum_i (\phi_i - \phi_{\boldsymbol{nh}_i})(\omega_i - \dot{\phi}_{\boldsymbol{nh}_i}) =$$

$$= \sum_i K[u_i] P_i + \sum_i \sum_{j \neq i} K[u_j] \nabla_j \Phi_i^\top \begin{bmatrix} \boldsymbol{J}_j \\ 0 \end{bmatrix} +$$

$$+ \sum_i K[w_i] \Phi_{iz} + \sum_i \sum_{j \neq i} K[w_j] \frac{\partial \Phi_i}{\partial z_j} - \sum_i \theta_i \dot{\theta}_i,$$

where $\theta_i = (\phi_i - \phi_{\mathbf{nhi}})$. By (7) we deduce:

$$\dot{\theta}_i = \begin{cases} -\dot{\phi}_{\mathbf{nhi}}, & M_i \geq \varepsilon_\phi \\ -\left[k_\phi \left(1 - \frac{M_i}{\varepsilon_\phi}\right) + \frac{\dot{\phi}_{\mathbf{nhi}}^2}{\varepsilon_\phi} \right] \cdot \theta_i, & 0 < M_i < \varepsilon_\phi \\ -k_\phi \theta_i, & M_i \leq 0. \end{cases}$$

We discriminate between the following three sets of agents:
$Q_1 \triangleq \left\{ i \in \{1, ., N\} \,\middle|\, \frac{\partial \Phi_i}{\partial t} - U_i |P_i| + U_i \varepsilon \leq 0 \right\}$
$Q_2 \triangleq \left\{ i \in \{1, ., N\} \,\middle|\, 0 < \frac{\partial \Phi_i}{\partial t} - U_i |P_i| + U_i \varepsilon \leq -\tilde{t}_i U_i \Phi_{iz} \right\}$
$Q_3 \triangleq \left\{ i \in \{1, ., N\} \,\middle|\, \frac{\partial \Phi_i}{\partial t} - U_i |P_i| + U_i \varepsilon > -\tilde{t}_i U_i \Phi_{iz} \right\}$
Similarly, we define the following non-intersecting sets:
$T_1 \triangleq \{i \in \{1, \ldots, N\} \,|\, M_i \geq \varepsilon_\phi \}$,
$T_2 \triangleq \{i \in \{1, \ldots, N\} \,|\, 0 < M_i < \varepsilon_\phi \}$,
$T_3 \triangleq \{i \in \{1, \ldots, N\} \,|\, M_i \leq 0 \}$.
By the control law (5) we deduce:

$$K[u_i] = \begin{cases} -K[s_i] \cdot U_i, & i \in Q_1 \bigcup Q_2 \\ -K[s_i] \frac{U_i \varepsilon + \frac{\partial \Phi_i}{\partial t}}{|P_i| - \tilde{t}_i \Phi_{iz}}, & i \in Q_3 \end{cases}$$

$K[w_i] = (1 - \min(\sigma_{\Phi i}, \sigma_{ni}, \sigma_{\alpha i})) \tilde{t}_i |u_i|$.
Note that $(1 - \min(\sigma_{\Phi i}, \sigma_{ni}, \sigma_{\alpha i})) \geq (1 - \sigma_{\Phi i}) \geq 0$ and $\tilde{t}_i \Phi_{iz} \leq 0$. Using control law (5a) and (3) we derive:

$$(1 - \sigma_{\Phi i}) = \begin{cases} 0, & i \in Q_1 \\ \frac{U_i(|P_i| - \varepsilon) - \frac{\partial \Phi_i}{\partial t}}{U_i \tilde{t}_i \Phi_{iz}} \in (0, 1], & i \in Q_2 \\ 1, & i \in Q_3. \end{cases}$$

Using the above, we proceed with $\dot{\tilde{V}}$:

$$\dot{\tilde{V}} = \sum_{Q_1 \bigcup Q_2} \left\{ -K[s_i] P_i U_i + \frac{\partial \Phi_i}{\partial t} \right\} +$$

$$+ \sum_{Q_3} \left\{ -K[s_i] P_i \frac{U_i \varepsilon + \frac{\partial \Phi_i}{\partial t}}{|P_i| - \tilde{t}_i \Phi_{iz}} + \frac{\partial \Phi_i}{\partial t} \right\} +$$

$$+ (1 - \min(\sigma_{\Phi i}, \sigma_{ni}, \sigma_{\alpha i})) \tilde{t}_i |u_i| \Phi_{iz} - \sum_{T_1} \theta_i \dot{\phi}_{\mathbf{nhi}} -$$

$$- \sum_{T_2} \left[k_\phi \left(1 - \frac{M_i}{\varepsilon_\phi}\right) + \frac{\dot{\phi}_{\mathbf{nhi}}^2}{\varepsilon_\phi} \right] \theta_i^2 - \sum_{T_3} k_\phi \theta_i^2 \leq$$

$$\leq \sum_{Q_1} \left\{ -|P_i| U_i + \frac{\partial \Phi_i}{\partial t} \right\} -$$

$$- \sum_{Q_2} \left\{ |P_i| U_i - \left(U_i (|P_i| - \varepsilon) - \frac{\partial \Phi_i}{\partial t} \right) - \frac{\partial \Phi_i}{\partial t} \right\} -$$

$$- \sum_{Q_3} \left\{ (|P_i| - \tilde{t}_i \Phi_{iz}) \frac{U_i \varepsilon + \frac{\partial \Phi_i}{\partial t}}{|P_i| - \tilde{t}_i \Phi_{iz}} - \frac{\partial \Phi_i}{\partial t} \right\} - \sum_{T_1} M_i -$$

$$- \sum_{T_2} \left\{ k_\phi \left(1 - \frac{M_i}{\varepsilon_\phi}\right) \theta_i^2 + \frac{M_i^2}{\varepsilon_\phi} \right\} - \sum_{T_3} k_\phi \theta_i^2 =$$

$$= \sum_{Q_1} \left\{ -|P_i| U_i + \frac{\partial \Phi_i}{\partial t} \right\} - \sum_{Q_2 \bigcup Q_3} U_i \varepsilon - \sum_{T_1} M_i$$

$$- \sum_{T_2} \left\{ k_\phi \left(1 - \frac{M_i}{\varepsilon_\phi}\right) \theta_i^2 + \frac{M_i^2}{\varepsilon_\phi} \right\} - \sum_{T_3} k_\phi \theta_i^2 \leq 0$$

Since each V_i, and consequently V, is regular [16] and the level sets of V are compact, the nonsmooth version of LaSalle's invariance principle [14] can be applied. Thus, the closed-loop system converges to the largest invariant subset S: $S \triangleq \left\{ \left[\mathbf{q}^\top, \phi \right]^\top \,\middle|\, 0 \in \dot{\tilde{V}} \right\}$. For the sets T_1, T_2 we deduce:

$$\sum_{T_1} M_i > 0, \quad \sum_{T_2} \left[k_\phi \left(1 - \frac{M_i}{\varepsilon_\phi}\right) \theta_i^2 + \frac{M_i^2}{\varepsilon_\phi} \right] > 0.$$

For $\dot{\tilde{V}} = 0$ to hold, all i must be in T_3, thus:
$S = \{\mathbf{n} : (|P_i| U_i - \frac{\partial \Phi_i}{\partial t} = 0 \forall i \in Q_1) \wedge (\varepsilon U_i = 0 \forall i \in Q_2) \wedge$
$\wedge (\theta_i = \phi_i - \phi_{\mathbf{nh}_i} = 0 \forall i)\}$.

Since $|P_i| U_i - \frac{\partial \Phi_i}{\partial t} \geq \varepsilon U_i \geq 0$, the equality must hold inside S, i.e. $U_i = 0$, requiring $\boldsymbol{q}_i = \boldsymbol{q}_{id}$ so that $\phi_i = \phi_{\mathbf{nh}_i} = \phi_{id} \forall i$. Thus, S reduces to the singleton $\{\mathbf{n} : (\boldsymbol{q}_i = \boldsymbol{q}_{id} \forall i) \wedge (\phi_i = \phi_{id} \forall i)\}$, i.e. all agents are stabilised to their destinations and desired orientations. ∎

VI. SIMULATION

We used our algorithm in a test case identical to the one in [3], consisting of 5 aircraft with converging straight line paths between their start and final positions. The desired horizontal velocity u_{id} of all agents was set to $5 \cdot 10^{-4}$, while the maximum climb and descent angles used were $\alpha_{iC} = 15^o$ and $\alpha_{iD} = -20^o$ respectively. Finally, the radius of all $\mathcal{C}_i$ and $\mathcal{S}_i$ was $c_i = 0.01$, $\theta_i^0 = 10^o$ and $\hat{\theta}_i = 15^o$. The resulting agents' paths are shown in Figure 5 while the horizontal linear (u_i) and angular velocity (ω_i) are depicted in Figure 6 and vertical velocities w_i are shown in Figure
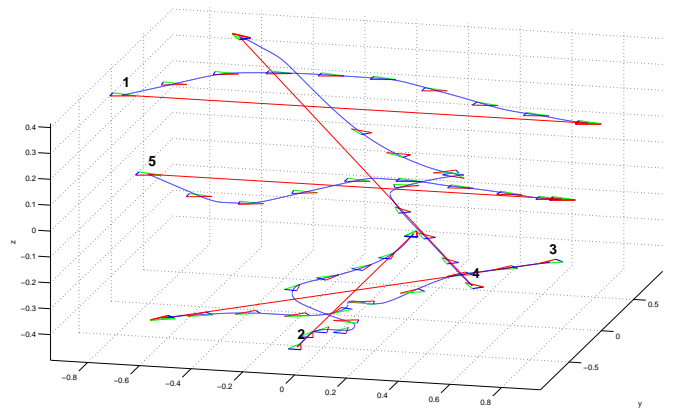

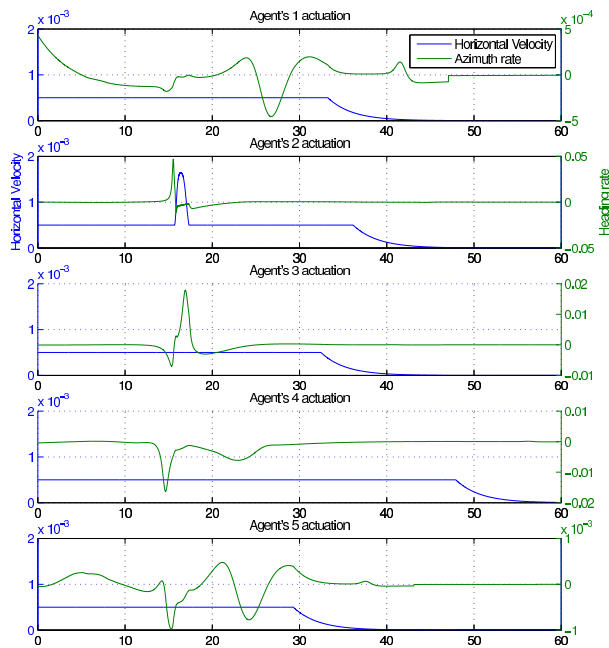Fig. 5. Aircraft's trajectories in 3D space
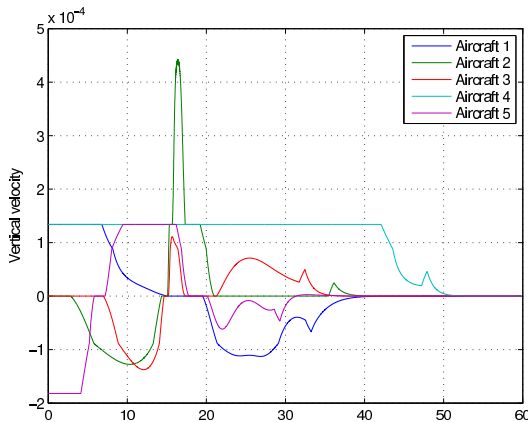
Fig. 6.   Horizontal and Angular Velocities

Fig. 7.   Vertical Velocities

7. All agents are driven towards their destination without colliding. Specifically, the following remarks can be made:

- All aircraft maintain their horizontal speed equal to the desired u_{id}, except for aircraft 2, which uses a higher speed only while avoiding a collision with aircraft 3.
- Aircraft fly mostly level, i.e. $w_i = 0$ and approach their destinations while their slope tends to 0.
- The bounded climb and descent angle combined with constant horizontal velocity results in bounded vertical velocity. When $\alpha_{\mathbf{nh}i}$ is saturated, $|\alpha_{\mathbf{nh}i}| > |\tilde{\alpha}_i|$ (beginning of aircraft 1 and 5 paths), and $|u_i| = u_{id}$, a constant vertical velocity is used, as in current ATC practice.
- The combined effects of the above remarks are obvious in aircraft's 1 *climb-fly level-descent* pattern.
- The initial and final positions of aircraft 4 result in a straight line path with climbing angle greater that α_{iC}. The aircraft performs a climbing circle to achieve the desired altitude while avoiding collision with aircraft 5.

VII. CONCLUSIONS

The control scheme presented here utilises the proven properties of Navigation Functions, for the control of aircraft-like agents in 3D space, while respecting aircraft's performance constraints. Compared to previous NF-based approaches, it yields results that more compatible with ATM practice and aircraft's constraints, while maintaining the formal guarantees of the NF framework. The proposed algorithm can be tuned via parameters representing practical limitations of aircraft (speed, climb and descent angle). Future work in this area focuses on further improving the compatibility of our algorithm with ATC applications, by incorporating curvature limits and further constraints.

VIII. ACKNOWLEDGEMENTS

REFERENCES

[1] G. Chaloulos, J. Lygeros, I. Roussos, K. Kyriakopoulos, E. Siva, A. Lecchini-Visintini, and P. Cásek, "Comparative study of conflict resolution methods," *iFLY Project, Deliverable D5.1*, June 2009.
[2] E. Rimon and D. E. Koditschek, "Exact robot navigation using artificial potential functions," *IEEE Transactions on Robotics and Automation*, vol. 8, no. 5, pp. 501–508, 1992.
[3] G. P. Roussos and K. J. Kyriakopoulos, "Towards constant velocity navigation and collision avoidance for autonomous nonholonomic aircraft-like vehicles," *Conference on Decision and Control*, 2009.
[4] G. C. Karras and K. Kyriakopoulos, "Visual servo control of an underwater vehicle using a laser vision system," *IEEE Intelligent Robots and Systems, Nice, France*, 2008.
[5] C. J. Tomlin, G. J. Pappas, and S. S. Sastry, "Conflict resolution for air traffic management: A study in multiagent hybrid systems," *IEEE Transactions on Automatic Control*, pp. 509–521, 1998.
[6] A. Bicchi and L. Pallottino, "On optimal cooperative conflict resolution for air traffic management systems," *IEEE Transactions on Intelligent Transportation Systems*, vol. 1, no. 4, pp. 221–231, 2000.
[7] G. Inalhan, D. Stipanovic, and C. Tomlin, "Decentralized optimization, with application to multiple aircraft coordination," *Proceedings of the 41st Conference on Decision and Control*, 2002.
[8] E. Lalish and K. A. Morgansen, "Decentralized reactive collision avoidance for multivehicle systems," *2008 IEEE Conference on Decision and Control*, 2008.
[9] H. G. Tanner, S. Loizou, and K. J. Kyriakopoulos, "Nonholonomic navigation and control of cooperating mobile manipulators," *IEEE Transactions on Robotics and Automation*, vol. 19, no. 1, pp. 53–64, 2003.
[10] D. V. Dimarogonas, S. G. Loizou, K. J. Kyriakopoulos, and M. M. Zavlanos, "A feedback stabilization and collision avoidance scheme for multiple independent non-point agents," *Automatica*, vol. 42, no. 2, pp. 229–243, 2006.
[11] S. G. Loizou, D. V. Dimarogonas, and K. J. Kyriakopoulos, "Decentralized feedback stabilization of multiple nonholonomic agents," *Proceedings of the 2004 International Conference on Robotics and Automation*, pp. 3012–3017, 2004.
[12] G. P. Roussos, D. V. Dimarogonas, and K. J. Kyriakopoulos, "Distributed 3D navigation and collision avoidance for multiple nonholonomic agents," *European Control Conference*, pp. 1830–1835, 2009.
[13] M. Egerstedt and X. Hu, "Formation constrained multi-agent control," *Robotics and Automation, IEEE Transactions on*, vol. 17, pp. 947–951, Dec 2001.
[14] D. Shevitz and B. Paden, "Lyapunov stability theory of nonsmooth systems," *IEEE Transactions on Automatic Control*, vol. 39, no. 9, pp. 1910–1914, 1994.
[15] A. Filippov, *Differential equations with discontinuous right-hand sides*. Kluwer Academic Publishers, 1998.
[16] F. Clarke, *Optimization and Nonsmooth Analysis*. Addison-Wesley, 1983.